



the society for solid-state  
and electrochemical  
science and technology

Journal of The Electrochemical Society

## Carbon Coated NASICON Type $\text{Li}_3\text{V}_{2-x}\text{M}_x(\text{PO}_4)_3$ (M=Mn, Fe and Al) Materials with Enhanced Cyclability for Li-Ion Batteries

J. N. Son, G. J. Kim, M. C. Kim, S. H. Kim, V. Aravindan, Y. G. Lee and Y. S. Lee

*J. Electrochem. Soc.* 2013, Volume 160, Issue 1, Pages A87-A92.  
doi: 10.1149/2.039301jes

---

### Email alerting service

Receive free email alerts when new articles cite this article - sign up in the box at the top right corner of the article or [click here](#)

---

---

To subscribe to *Journal of The Electrochemical Society* go to:  
<http://jes.ecsdl.org/subscriptions>

---



## Carbon Coated NASICON Type $\text{Li}_3\text{V}_{2-x}\text{M}_x(\text{PO}_4)_3$ (M=Mn, Fe and Al) Materials with Enhanced Cyclability for Li-Ion Batteries

J. N. Son,<sup>a</sup> G. J. Kim,<sup>a</sup> M. C. Kim,<sup>a</sup> S. H. Kim,<sup>a</sup> V. Aravindan,<sup>a,b</sup> Y. G. Lee,<sup>c</sup> and Y. S. Lee<sup>a,z</sup>

<sup>a</sup>Faculty of Applied Chemical Engineering, Chonnam National University, Gwang-ju 500-757, Korea

<sup>b</sup>Energy Research Institute @ NTU (ERI@N), Nanyang Technological University, Research Techno Plaza, Singapore 637553, Singapore

<sup>c</sup>Convergence and Components & Materials Research Lab., Electronics and Telecommunications Research Institute, Daejeon 305-700, Korea

We report the synthesis and optimization of metal (Mn, Fe and Al) doped NASICON type  $\text{Li}_3\text{V}_2(\text{PO}_4)_3$  by solid-state reaction method. Among the metal doping, 0.02 mol concentration of Al is found better performing electrode while approaching the removal of three moles of lithium between 3–4.8 V vs. Li. Adipic acid with various concentrations is used to generate in-situ carbon layer over the 0.02 mol Al doped  $\text{Li}_3\text{V}_2(\text{PO}_4)_3$  particulates ( $\text{Li}_3\text{V}_{1.98}\text{Al}_{0.02}(\text{PO}_4)_3$ ). Presence of carbon on the surface of particulates is confirmed by TEM and Raman analysis. Half-cell Li/C- $\text{Li}_3\text{V}_{1.98}\text{Al}_{0.02}(\text{PO}_4)_3$  (0.15 mol of adipic acid) exhibited the highest reversible capacity of  $\sim 182 \text{ mAh g}^{-1}$  (2.77 moles of lithium) at a current density of  $0.1 \text{ mA cm}^{-2}$  compared to rest of the adipic acid concentrations. Further, the cell retained 83% of capacity after 50 galvanostatic charge-discharge cycles at ambient conditions. Li-insertion/extraction mechanism and improvement in electronic conductivity profiles are validated through cyclic voltammetry and electrochemical impedance spectroscopy, respectively.

© 2012 The Electrochemical Society. [DOI: 10.1149/2.039301jes] All rights reserved.

Manuscript submitted July 16, 2012; revised manuscript received October 15, 2012. Published November 12, 2012.

In the recent past, research focus has been devoted to the development of high performance lithium-ion batteries (LIB) to power hybrid electric vehicles (HEV) and electric vehicles (EV).<sup>1–4</sup> To realize these goals, high energy density Li-ion battery packs having high capacity and high voltage cathode materials with much more safety features than conventional cathodes are warranted.<sup>5</sup> Commercially available layered type materials  $\text{LiCoO}_2$ ,  $\text{LiNiO}_2$ ,  $\text{LiNi}_{1/3}\text{Co}_{1/3}\text{Mn}_{1/3}\text{O}_2$  and spinel  $\text{LiMn}_2\text{O}_4$  cathodes experience poor thermal stability particularly in de-lithiated state, which hinders the possibility of using them in high energy density practical LIBs. Under abusive conditions, those materials evolve  $\text{O}_2$ , which leads to the thermal runaway of the battery. Since the discovery of reversible Li-insertion/extraction in polyanion framework materials especially  $\text{LiFePO}_4$  by Padhi et al.,<sup>6</sup> several research work have been reported on such polyanion framework materials, particularly  $(\text{PO}_4)^{3-}$  anions, due to its thermal stability in both lithiated/de-lithiated states, because of the existence of strong P–O co-valent bond.<sup>6–11</sup> Further, such polyanions enable very flat charge/discharge profiles due to the inductive effect attributed to a two-phase reaction mechanism. Taking the mentioned advantages of  $(\text{PO}_4)^{3-}$  group, rest of the polyanion olivine family framework materials such as  $\text{LiMnPO}_4$ ,  $\text{LiCoPO}_4$  and  $\text{LiNiPO}_4$  were reported as prospective cathodes.<sup>12</sup> However, except for  $\text{LiMnPO}_4$ , rest of the materials showed redox potentials ( $\sim 4.8 \text{ V}$  for  $\text{LiCoPO}_4$  and  $\sim 5.2 \text{ V}$  for  $\text{LiNiPO}_4$ ) higher than the thermodynamical stability window of the conventional electrolyte ( $\sim 4.6 \text{ V}$  vs. Li). For the case of  $\text{LiMnPO}_4$ , few groups achieved only a practical capacity of  $> 150 \text{ mAh g}^{-1}$  at operating potential of  $4.1 \text{ V}$  vs. Li.<sup>13</sup> On the other hand, NASICON framework materials, similar to olivine family, comprising the general formula  $\text{A}_x\text{M}_2(\text{XO}_4)_3$ , where  $\text{A}=\text{Na}$  or  $\text{Li}$ ;  $\text{M}=\text{Ti}$ ,  $\text{V}$ ,  $\text{Fe}$  and  $\text{X}=\text{P}$ ,  $\text{S}$ ,  $\text{Mo}$ ,  $\text{W}$ ,  $\text{As}$ , are also attractive as prospective electrode materials for LIB applications.<sup>4</sup> NASICON type materials consist of  $\text{MO}_6$  octahedral units sharing all their corners with  $\text{XO}_4$  tetrahedra. However, the  $\text{XO}_4$  tetrahedral units share all three corners with  $\text{MO}_6$  octahedra. This enables the generation of interstitial and conduction channels along the  $c$ -axis direction, in which alkali metal ions ( $\text{Na}^+$  or  $\text{Li}^+$ ) can occupy the interstitial position. This enables three dimensional Li-ion pathways for Li-insertion during electrochemical cycling, unlike that in olivine framework materials, in which one dimensional migration is reported.<sup>14</sup> Among the NASICON type materials reported,  $\text{Li}_3\text{V}_2(\text{PO}_4)_3$  is promising with the maximum theoretical capacity of  $197 \text{ mAh g}^{-1}$  (among the phosphate anions) for the removal of three moles of lithium. However, achieving the theoretical capacity is too

complicated in such framework materials due to the distorted arrangement of  $\text{VO}_6$  octahedral units which results in poor electronic conductivity. Apart from the inherent conductivity issues,  $\text{Li}_3\text{V}_2(\text{PO}_4)_3$  material undergoes structural destruction while removing the third Li-ion from the lattice and it leads to severe capacity fading during cycling.<sup>12</sup> Vanadium site doping and carbon coating are expected to suppress structural destruction and overcome the inherent conductivity issues, respectively. So far, few reports are available on the carbon coating and metal doping on NASICON type  $\text{Li}_3\text{V}_2(\text{PO}_4)_3$  and there have been no reports on appropriate optimization studies. More importantly, most of the work reported are restricted to the removal of two moles of Li-ions and there are no comprehensive studies on the removal of third Li-ion.<sup>12</sup> In addition to the suppression of structural destruction, partial substitution of Vanadium also increases the ionic conductivity of NASICON type compound as well. In this study, an attempt has been made to synthesize in-situ carbon coated  $\text{Li}_3\text{V}_{2-x}\text{M}_x(\text{PO}_4)_3$  with various metal ions ( $\text{M}=\text{Mn}$ ,  $\text{Fe}$  and  $\text{Al}$ ) under the optimized conditions. For the carbon coating, choice of precursor is important to achieve high performance electrodes. Generally, carboxylic acids are found promising for in-situ coating process because of such advantages as easy carbonization and formation of carbon layer over the surface of particulates during synthesis, and presence of  $-\text{COOH}-$  groups, which effectively prevents particle growth during high temperature synthesis, particularly in solid-state reaction.<sup>15–17</sup> In the present case, adipic acid, a di-carboxylic acid, is used as the source for carbon. Extensive studies on the preparation and electrochemical characterization of transition metal substituted NASICON type  $\text{Li}_3\text{V}_2(\text{PO}_4)_3$  have been carried out and results are described in detail.

### Experimental

Metal substituted  $\text{Li}_3\text{V}_{2-x}\text{M}_x(\text{PO}_4)_3$ , where  $\text{M}=\text{Mn}$ ,  $\text{Fe}$  and  $\text{Al}$  phases were synthesized by conventional solid-state route under the optimized temperature conditions. The optimized temperature conditions are as follows; pre-calcination at  $300^\circ\text{C}$  for 4 h in air and  $900^\circ\text{C}$  for 8 h under Ar atmosphere to yield high performance NASICON type materials. Analytical grade  $\text{Li}_2\text{CO}_3$  (Wako, Japan),  $\text{V}_2\text{O}_5$  (Sigma-Aldrich, USA),  $(\text{NH}_4)_2\text{HPO}_4$  (Sigma-Aldrich, USA),  $\text{Fe}_2\text{O}_3$ ,  $\text{Al}(\text{OH})_3$  and  $\text{Mn}_3\text{O}_4$  were purchased and used as such. In the typical synthesis procedure, stoichiometric amounts of  $\text{Li}_2\text{CO}_3$ ,  $\text{V}_2\text{O}_5$ , and  $(\text{NH}_4)_2\text{HPO}_4$  were finely ground in an agate mortar and calcined at  $400^\circ\text{C}$  for 4 h in air using a box furnace for the decomposition of hydroxyl and ammonium moieties. The intermediate product was harvested and ground again to form a pellet and fired at  $900^\circ\text{C}$  for 8 h under Ar flow to yield a single phase  $\text{Li}_3\text{V}_{2-x}\text{M}_x(\text{PO}_4)_3$ ,

<sup>z</sup>E-mail: leeyes@chonnam.ac.kr

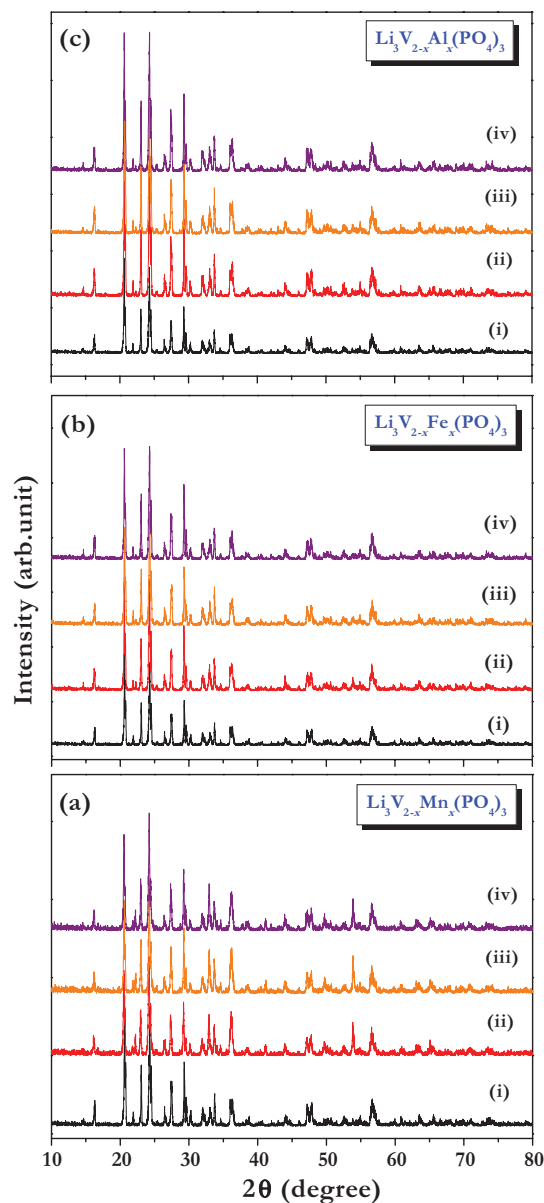
where  $M = \text{Mn, Fe and Al}$  with desired composition. The same procedure was repeated for in-situ carbon coating using adipic acid as the precursor by tuning the concentration of precursor under the optimized synthesis conditions mentioned above.

Powder X-ray diffractometer equipped with  $\text{CuK}\alpha$  radiation (XRD, Rint 1000, Rigaku, Japan) was used to analyze the structural properties of  $\text{Li}_3\text{V}_{2-x}\text{M}_x(\text{PO}_4)_3$  phase. Internal structure of the carbon coated NASICON type compound was investigated through transmission electron microscopy (TEM, TECNAI, Philips, Netherlands). Electrochemical Li-insertion properties were evaluated in standard two-electrode CR 2032 coin-cell configuration. Test electrodes were formulated with accurately weighed 20 mg of NASICON type active material, 3 mg of Ketjen black and 3 mg of Teflonized acetylene black, TAB-2. The composite film was formed and pressed on a 200  $\text{mm}^2$  stainless steel mesh, which served as the current collector. Then, electrodes were dried at  $160^\circ\text{C}$  for 4 h in a vacuum oven before conducting cell assembly in Ar filled glove box. The test cells were constructed with a composite cathode and metallic lithium as anode, separated by a porous polypropylene film (Celgard 3401, USA). 1 M  $\text{LiPF}_6$  in ethylene carbonate:dimethyl carbonate (1:1 by vol.) was used as electrolyte solution obtained from Techno Semichem Co., Ltd., Korea. Cyclic voltammetry (CV) and electrochemical impedance spectroscopy (EIS) were conducted by two-electrode setup using a Bio-Logic electrochemical work station (SP-150, Biologic, France), in which metallic lithium acts as both working and counter electrode. Galvanostatic cycling studies were carried out between 3–4.8 V with different current densities in ambient temperature conditions.

## Results and Discussion

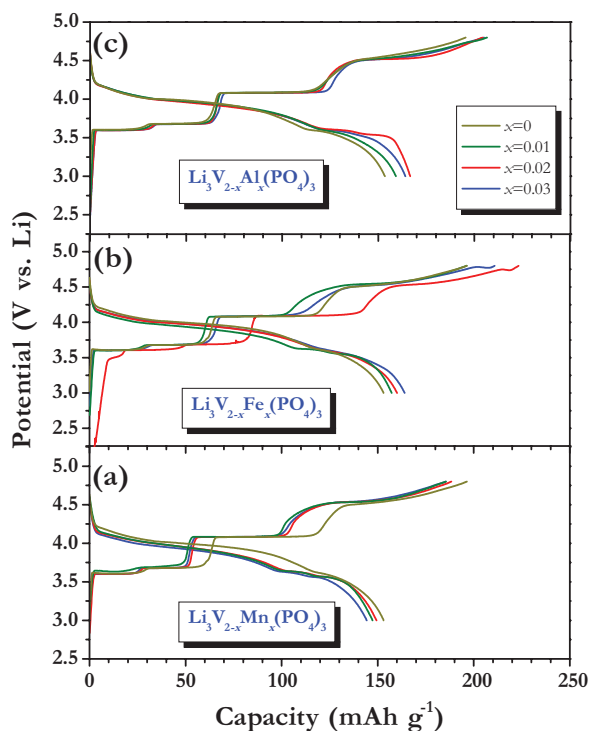
Powder X-ray diffraction (XRD) pattern of NASICON type  $\text{Li}_3\text{V}_{2-x}\text{M}_x(\text{PO}_4)_3$ , where  $M = \text{Mn, Fe and Al}$  with different concentrations along with pristine material is given in Figure 1. The figure clearly shows the formation of a single phase material and absence of impurity traces like,  $\text{Li}_3\text{PO}_4$ ,  $\text{V}_2\text{O}_3$ ,  $\text{V}_2\text{O}_5$  etc. The observed reflections belong to monoclinic structure with  $P2_1/n$  space group. Further, there is no deviation in the peak positions and there are no peaks corresponding to either Mn, Fe or Al. This is mainly due to the fact that the amount of transition metal doping is too low for detection by X-ray diffraction instrument. It is well known that, the structure of NASICON type  $\text{Li}_3\text{V}_{2-x}\text{M}_x(\text{PO}_4)_3$  consists of a three-dimensional framework of metal octahedra ( $\text{VO}_6$ ) units and phosphate tetrahedral ( $\text{PO}_4$ ) units sharing oxygen vertices. Each  $\text{VO}_6$  octahedral unit is surrounded by six  $\text{PO}_4$  tetrahedral units. However, each tetrahedral unit is surrounded by four  $\text{VO}_6$  octahedral units. This configuration forms a three-dimensional network and the alkali cation, Li, is located in the cavities within the framework.<sup>7</sup> Three four-fold crystallographic positions exist for the lithium atoms, leading to twelve lithium positions within the unit-cell. All the phases prepared with various metal ion substitution on Vanadium site yields single phase material. Therefore, high performance electrode material was chosen based on the Li-insertion properties in half-cell configuration to employ subsequent studies and carbon coating.

Figure 2 illustrates the galvanostatic charge-discharge curves of NASICON type  $\text{Li}_3\text{V}_{2-x}\text{M}_x(\text{PO}_4)_3$  powders in half-cell configuration and cycled between 3–4.8 V vs. Li at current density of  $0.1 \text{ mA cm}^{-2}$  in ambient temperature conditions. It is obvious from the charge-discharge profiles that the charge capacity is higher than discharge capacity irrespective of the metal ion doping (which is mainly due to the extraction of more than two moles of Li) and decomposition of solvent molecules as well. Theoretically,  $\sim 132 \text{ mAh g}^{-1}$  corresponds to the removal of two moles of lithium from  $\text{Li}_3\text{V}_{2-x}\text{M}_x(\text{PO}_4)_3$  lattice. Extraction of third lithium from the crystal lattice takes place at  $\sim 4.6 \text{ V}$ , which is the maximum thermodynamical stability window of the conventional carbonate based electrolytes. The reversible capacity of more than  $150 \text{ mAh g}^{-1}$  was recorded for all the compositions tested in half-cell configuration and it confirms the reversible insertion/extraction of more than two moles of lithium. The cell  $\text{Li}/\text{Li}_3\text{V}_{2-x}\text{Mn}_x(\text{PO}_4)_3$ , delivered the initial discharge capacity of



**Figure 1.** Powder X-ray diffraction pattern of (a)  $\text{Li}_3\text{V}_{2-x}\text{Mn}_x(\text{PO}_4)_3$ , (b)  $\text{Li}_3\text{V}_{2-x}\text{Fe}_x(\text{PO}_4)_3$  and (c)  $\text{Li}_3\text{V}_{2-x}\text{Al}_x(\text{PO}_4)_3$ , where  $0 \leq x \leq 0.03$ , in which (i) 0, (ii) 0.01, (iii) 0.02 and (iv) 0.03.

152, 149, 147 and 153  $\text{mAh g}^{-1}$  for  $x$  values of 0, 0.01, 0.02 and 0.03, respectively. Discharge capacity of 157, 160 and 164  $\text{mAh g}^{-1}$  was found for Fe doping for molar concentrations of 0.01, 0.02 and 0.03, respectively. In the case of Al doping, test cells displayed the reversible capacity of 159, 166 and 164  $\text{mAh g}^{-1}$  for the molar concentrations of 0.01, 0.02 and 0.03, respectively. Charge-discharge curves of neat and doped compounds involve multiple redox steps which correspond to the Li-extraction/insertion reactions at various levels. Removal of first lithium takes place according to the two-phase reaction in two step process at  $\sim 3.6 \text{ V}$  ( $\text{Li}_{2.5}\text{V}_2^{3+/4+}(\text{PO}_4)_3$ ) and  $\sim 3.7 \text{ V}$  ( $\text{Li}_2\text{V}_2^{3+/4+}(\text{PO}_4)_3$ ). At  $\sim 4.1 \text{ V}$  extraction of second lithium takes place ( $\text{Li}_1\text{V}_2^{4+}(\text{PO}_4)_3$ ), which preserves the monoclinic symmetry of the lattice.<sup>18</sup> Well-defined, long distinct plateau at  $\sim 4.1 \text{ V}$  corresponds to the bi-phase reaction and is associated with  $\text{V}^{3+/4+}$  redox couple. The third and final lithium removal occurred at  $\sim 4.55 \text{ V}$  ( $\text{Li}_0\text{V}_2(\text{PO}_4)_3$ ), at which vanadium is in a mixed valence state of  $\text{V}^{4+}$  and  $\text{V}^{5+}$ . Overall removal of lithium showed well defined plateaus in all the levels, whereas during the discharge process



**Figure 2.** Galvanostatic charge-discharge curves of various metal ion doping on vanadium site (a)  $\text{Li}_3\text{V}_{2-x}\text{Mn}_x(\text{PO}_4)_3$ , (b)  $\text{Li}_3\text{V}_{2-x}\text{Fe}_x(\text{PO}_4)_3$  and (c)  $\text{Li}_3\text{V}_{2-x}\text{Al}_x(\text{PO}_4)_3$ , where  $0 \leq x \leq 0.03$  cycled between 3–4.8 V vs. Li at current density of  $0.1 \text{ mA cm}^{-2}$ .

the  $\text{Li}_3\text{V}_2(\text{PO}_4)_3$  phase exhibits peculiarity than Li-extraction process. More specifically, charging process is composed of well-defined plateaus and it corresponds to the two-phase reaction, whereas during discharge monotonous curves are obtained and it is associated with solid-solution formation. During the reversible insertion of the first two lithium ions, a monotonous curve is noted ( $\text{Li}_0\text{V}_2(\text{PO}_4)_3 \rightarrow \text{Li}_2\text{V}_2(\text{PO}_4)_3$ ), which indicates the formation of solid-solution.<sup>18,19</sup> On the other hand, re-insertion of third lithium implies a two-phase reaction in a two-step process at  $\sim 3.55 \text{ V vs. Li}$  ( $\text{Li}_2\text{V}_2(\text{PO}_4)_3 \rightarrow \text{Li}_{2.5}\text{V}_2(\text{PO}_4)_3$ ) and  $\sim 3.6 \text{ V vs. Li}$  ( $\text{Li}_{2.5}\text{V}_2(\text{PO}_4)_3 \rightarrow \text{Li}_3\text{V}_2(\text{PO}_4)_3$ ), which is similar to first lithium-extraction. Most of the reports available on the NASICON type  $\text{Li}_3\text{V}_2(\text{PO}_4)_3$  compounds are mainly restricted to the removal of two moles of lithium (upper cutoff potential is restricted to 4.3 V vs. Li) and ensure reversible two-phase reaction without damaging crystal lattice while removing third lithium. Galvanostatic cycling studies were continued for few more cycles (minimum of 10 cycles) to identify the best performing compositions. The cycling profiles of NASICON type powders with different metal doping are illustrated in Figure 3. It shows, discharge capacities above  $150 \text{ mAh g}^{-1}$  is noted for Fe and Al doping, whereas Mn resulted in the poor capacity profiles irrespective of the concentration. In addition all the compositions experience capacity fade during cycling. In addition to structural destruction while testing above 4.3 V vs. Li several factors are believed for such cause likely as vanadium dissolution, electrolyte decomposition and inherent conductivity issues.<sup>3,20,21</sup> After 10 cycles, there is no significant difference in the cycling profiles for Fe doping and delivered the discharge capacity of 131, 128 and  $133 \text{ mAh g}^{-1}$  for 0.01, 0.02 and 0.03 molar concentrations, respectively were recorded. The observed values correspond to capacity retention of 83, 80 and 81% of its initial discharge capacity for 0.01, 0.02 and 0.03 molar concentrations, respectively. For the case of Mn doping, reversible capacities of 111, 105 and  $106 \text{ mAh g}^{-1}$  are observed for molar concentrations of 0.01, 0.02 and 0.03. On the other hand, Al doping enables good cycling profiles when compared to the Fe and Mn doping and test cells displayed the discharge capacity of

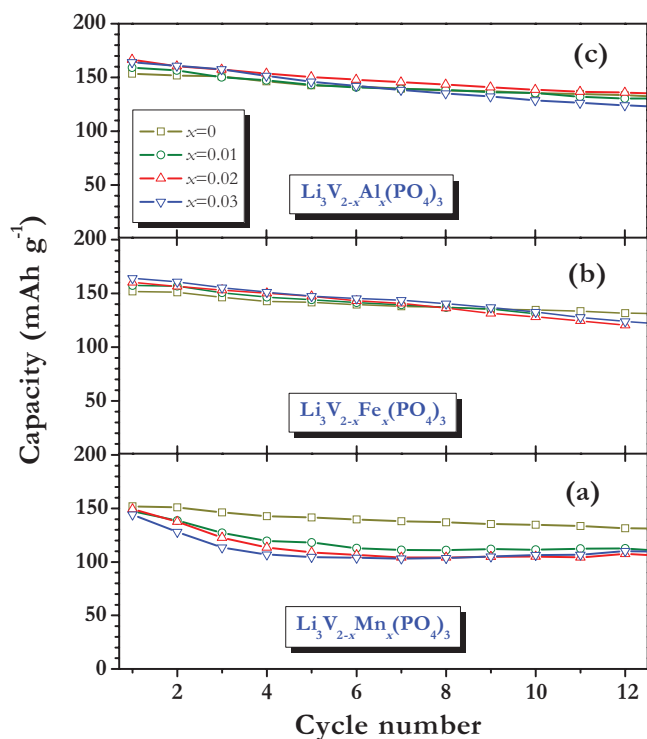


**Figure 3.** Galvanostatic cycling profiles of various metal ion doping on vanadium site (a)  $\text{Li}_3\text{V}_{2-x}\text{Mn}_x(\text{PO}_4)_3$ , (b)  $\text{Li}_3\text{V}_{2-x}\text{Fe}_x(\text{PO}_4)_3$  and (c)  $\text{Li}_3\text{V}_{2-x}\text{Al}_x(\text{PO}_4)_3$ , where  $0 \leq x \leq 0.03$  cycled between 3–4.8 V vs. Li in ambient temperature conditions.

135, 139 and  $129 \text{ mAh g}^{-1}$  for 0.01, 0.02 and 0.03 molar concentrations, respectively. Among the 10 compositions of  $\text{Li}_3\text{V}_{2-x}\text{M}_x(\text{PO}_4)_3$  ( $\text{M}=\text{Mn, Fe and Al}$ ) tested,  $\text{Li}_3\text{V}_{1.98}\text{Al}_{0.02}(\text{PO}_4)_3$  is found promising in terms of its higher reversible capacity and good cyclability. Further, it is well known that Al doping provides good electrochemical performance at elevated temperature operations, stabilizes the crystal structure during Li-insertion/extraction, in low cost and environmentally benign.<sup>22,23</sup> Thus, to take the advantage of Al doping, NASICON type  $\text{Li}_3\text{V}_{1.98}\text{Al}_{0.02}(\text{PO}_4)_3$  phase was subjected to the in-situ carbon coating process.

XRD patterns of  $\text{Li}_3\text{V}_{1.98}\text{Al}_{0.02}(\text{PO}_4)_3$  compounds synthesized along with different molar concentrations of adipic acid is given in Figure 4. Molar concentration of the adipic acid is fixed based on the

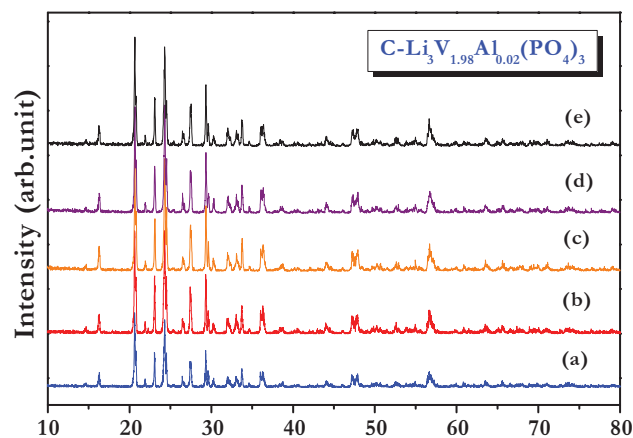


**Figure 4.** Powder X-ray diffraction pattern of NASICON type  $\text{Li}_3\text{V}_{1.98}\text{Al}_{0.02}(\text{PO}_4)_3$  with different molar concentration of adipic acid (a) 0, (b) 0.05, (c) 0.1, (d) 0.15 and (e) 0.2.



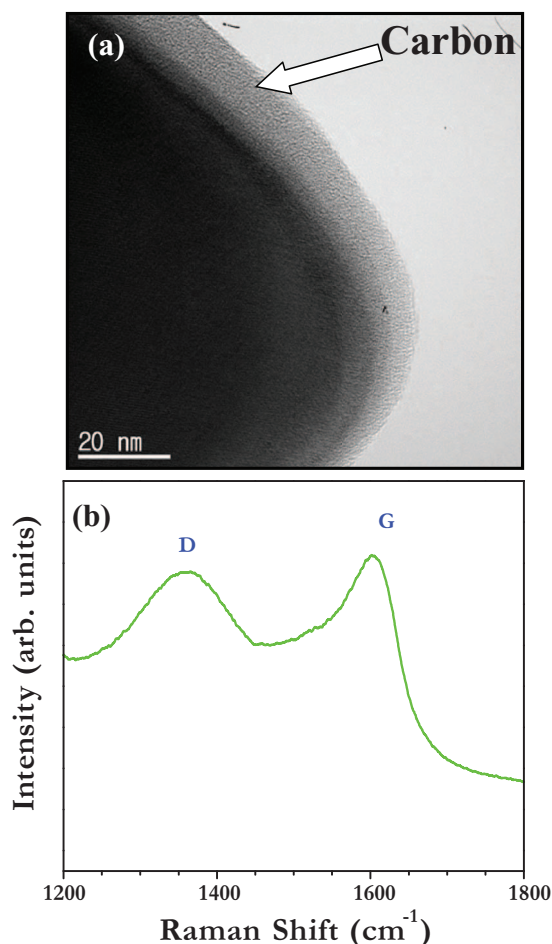


**Figure 5.** (a) High resolution transmission electron microscopy images of NASICON type carbon coated  $\text{Li}_3\text{V}_{1.98}\text{Al}_{0.02}(\text{PO}_4)_3$  powders with adipic acid concentration of 0.15 mol (b) Raman spectra of  $\text{C-Li}_3\text{V}_{1.98}\text{Al}_{0.02}(\text{PO}_4)_3$  (0.15 mol Adipic acid concentration).

total metal ion present the compound. The observed XRD reflections clearly reveal the formation of single phase NASICON type compounds. On the other hand, there are no reflections corresponding to the carbon which is due to low content of in-situ formed carbon which is too small for the detectable limitations of X-ray diffractometer. Apart from the amount of carbon present in the  $\text{Li}_3\text{V}_{1.98}\text{Al}_{0.02}(\text{PO}_4)_3$ , the nature of in-situ formed carbon is found amorphous. To monitor the presence of carbon and nature of the such layer formed over the surface of the carbon coated  $\text{Li}_3\text{V}_{1.98}\text{Al}_{0.02}(\text{PO}_4)_3$  (hereafter abbreviated as  $\text{C-Li}_3\text{V}_{1.98}\text{Al}_{0.02}(\text{PO}_4)_3$ ) particulates, transmission electron microscopy (TEM) and Raman analysis were performed and presented in Figure 5. For the said investigation only selected composition for example 0.15 mol adipic acid treated one was chosen. The TEM picture clearly reveals presence of carbon layer with the thickness of  $\sim 12$  nm. Characteristic Raman bands in  $\text{C-Li}_3\text{V}_{1.98}\text{Al}_{0.02}(\text{PO}_4)_3$  at  $\sim 1360$  and  $\sim 1600$   $\text{cm}^{-1}$  were ascribed to D and G modes, respectively.<sup>24</sup> Generally, D and G modes are attributed to the disordered and graphitic forms of carbon, respectively. Intensity ratio between D and G modes provides information about the degree of crystallinity of in-situ generated carbon and found to be 0.94, which clearly suggest the presence of dominant  $sp^2$  type carbon, thereby enabling good electronic conductivity profiles.<sup>11</sup> Therefore, good electrochemical performances are expected for the  $\text{C-Li}_3\text{V}_{1.98}\text{Al}_{0.02}(\text{PO}_4)_3$  compounds irrespective of the concentration of adipic acid used.

Electrochemical Li-insertion properties of  $\text{C-Li}_3\text{V}_{1.98}\text{Al}_{0.02}(\text{PO}_4)_3$  were evaluated in half-cell configuration between 3–4.8 V at constant current density of  $0.1 \text{ mA cm}^{-2}$  at room temperature.

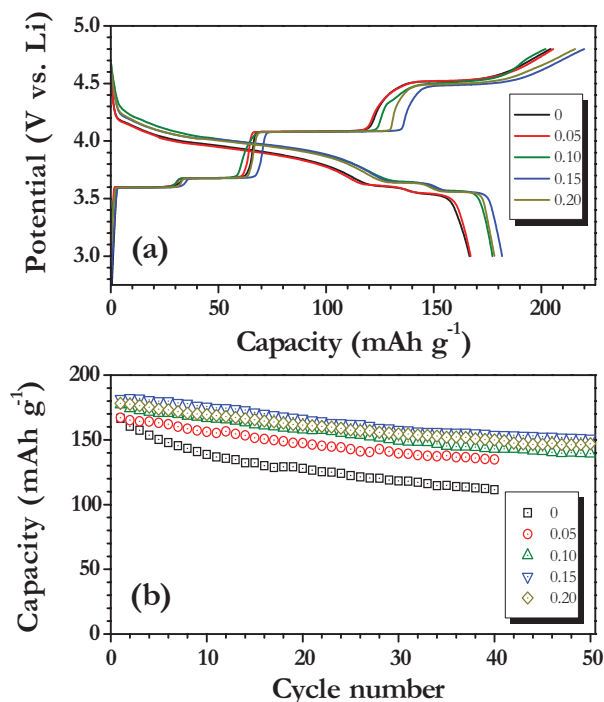
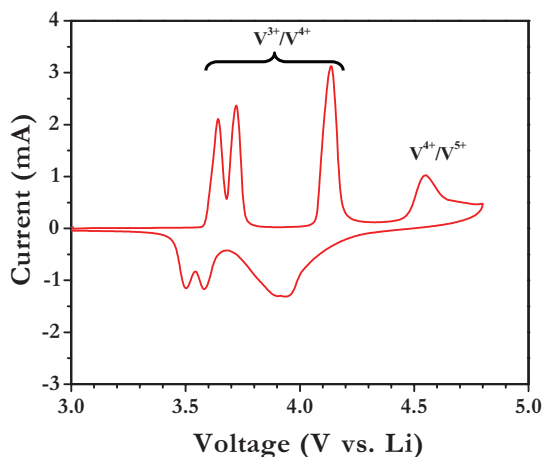


**Figure 6.** (a) Initial charge-discharge curves of NASICON type  $\text{Li}_3\text{V}_{1.98}\text{Al}_{0.02}(\text{PO}_4)_3$  with different molar concentration of adipic acid and (b) Plot of discharge capacity vs. cycle number.

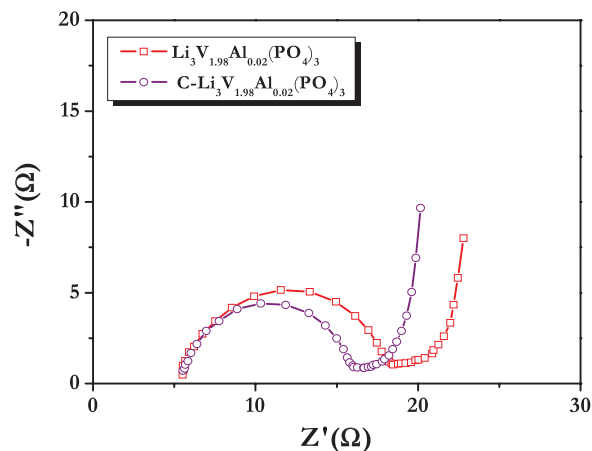
First charge-discharge curves of  $\text{Li/C-Li}_3\text{V}_{1.98}\text{Al}_{0.02}(\text{PO}_4)_3$  half-cells with different adipic acid concentration is illustrated in Figure 6a. The cells delivered discharge capacity of 167, 167, 179, 182 and 178  $\text{mAh g}^{-1}$  for adipic acid concentration of 0, 0.05, 0.1, 0.15 and 0.2 moles, respectively. It is clear that good improvement in the reversible insertion of Li-ions is observed in first discharge when compared to  $\text{Li}_3\text{V}_{1.98}\text{Al}_{0.02}(\text{PO}_4)_3$ . Maximum reversible insertion of 2.77 moles of lithium can be achieved for 0.15 mole adipic acid concentration. Increasing adipic acid concentration (0 to 0.15 mol) during synthesis process leads to higher reversible capacity (167 to 182  $\text{mAh g}^{-1}$ ). When the adipic acid concentration exceeds beyond 0.15 mol the reversible capacity tends to decrease, which is mainly due to the formation of larger amount of carbon content which subsequently dilutes the active material distribution. Lower content of adipic acid (0.05 mol) also exhibited poor capacity profiles and the concentration is not sufficient to improve the conductivity for desired performance. This clearly indicates that improved electrochemical performance is mainly attributed to the optimization of carbon content which enhances electronic conductivity of the NASICON type  $\text{Li}_3\text{V}_{1.98}\text{Al}_{0.02}(\text{PO}_4)_3$  phase by achieving higher reversible capacities. In addition to above, choice of precursor material for carbon is also very critical to obtain high performance in-situ generated carbon layers to improve electrochemical properties of such polyanion framework materials. Recently, Fey et al.<sup>15</sup> investigated utilization of various types of carboxylic acids such as malonic acid, adipic acid, sebacic acid, salicylic acid and ascorbic acid as a source material to generate in-situ carbon layer on polyanion framework  $\text{LiFePO}_4$  and found that adipic acid yields higher reversible capacity with less amount of precursor concentration than other and subsequently reduces production cost. Taking this advantage of adipic acid, we optimized the concentration to attain high performance NASICON type polyanion framework,  $\text{Li}_3\text{V}_{1.98}\text{Al}_{0.02}(\text{PO}_4)_3$ . Apart from the NASICON type materials, we already demonstrated the enhanced electrochemical performance of other polyanion hosts such as  $\text{LiFePO}_4$ ,  $\text{Li}_2\text{MnSiO}_4$  and  $\text{LiMnBO}_3$  by using adipic acid as the source material for carbon.<sup>17,25–28</sup> Plot of discharge capacity vs. cycle number of  $\text{C-Li}_3\text{V}_{1.98}\text{Al}_{0.02}(\text{PO}_4)_3$  phase is presented in

Figure 6b. A noticeable difference in the electrochemical profiles of  $\text{Li}_3\text{V}_{1.98}\text{Al}_{0.02}(\text{PO}_4)_3$  phases are evident. Adipic acid concentration of 0.1, 0.15 and 0.2 exhibits good electrochemical cyclability with different values compared to bare and 0.05 mol concentration. The 0.15 mol adipic acid carbonized during synthesis of  $\text{Li}_3\text{V}_{1.98}\text{Al}_{0.02}(\text{PO}_4)_3$  phase exhibited good capacity retention of 85% after 40 cycles compared to rest of the concentrations (67% for 0, 81% for 0.05, 81% for 0.1 and 83% for 0.2 mol of adipic acid). This clearly reveals that introduction of carbon coating not only provides an improvement in the electronic conductivity but it also prevents unwanted side reaction with electrolyte solutions. Further, these results are one of the best results obtained in NASICON framework materials for the removal of three moles of lithium. For example, Ko et al.<sup>29</sup> reported spray pyrolysed  $\text{C-Li}_3\text{V}_2(\text{PO}_4)_3$  with reversible capacity of  $141 \text{ mAh g}^{-1}$  at 0.1 C rate between 3–4.8 V.  $\text{Li}_3\text{V}_2(\text{PO}_4)_3$ -graphene composite was reported by Liu et al.<sup>30</sup> and test cell delivered the reversible capacity of  $\sim 165 \text{ mAh g}^{-1}$  at 0.1 C rate in the above potential window. Fu et al.<sup>31</sup> reported solid-state synthesized  $\text{C-Li}_3\text{V}_2(\text{PO}_4)_3$  and delivered a discharge capacity of  $\sim 137 \text{ mAh g}^{-1}$  at 1 C rate. Solution processed  $\text{C-Li}_3\text{V}_2(\text{PO}_4)_3$  composites are reported by Tang et al.<sup>32</sup> and presented the reversible capacities of  $164 \text{ mAh g}^{-1}$  at 0.2 C rate. Such a good reversible Li-insertion/extraction makes the compounds attractive for developing safer and higher energy density LIBs for possible application in HEV and EV.

Cyclic voltammetry (CV) study was conducted in the 3–4.8 V range at scan rate of  $0.05 \text{ mV s}^{-1}$  in two electrode coin-cell configurations to validate the reaction mechanism described above. Typical CV signatures of  $\text{C-Li}_3\text{V}_{1.98}\text{Al}_{0.02}(\text{PO}_4)_3$  in half-cell configuration is illustrated in Fig. 7. In the charge process, appearance of very sharp peaks at  $\sim 3.65$  and  $\sim 3.73 \text{ V}$  vs. Li are evident, which correspond to the extraction of one mole lithium (oxidation of  $\text{V}^{3+}$  to  $\text{V}^{4+}$  with two levels). Another sharp oxidation peak at  $\sim 4.14 \text{ V}$  is ascribed to the removal of second lithium from the lattice (complete oxidation of  $\text{V}^{3+}$  to  $\text{V}^{4+}$ ). Oxidation potential at  $\sim 4.48 \text{ V}$  vs. Li associated with the removal of third lithium to form  $\text{Li}_0\text{V}_2(\text{PO}_4)_3$ . The well defined oxidation peak during charge process associated with two-phase reaction was evident from the flat potential region during galvanostatic cycling. The broad potential is mainly ascribed to formation of solid-solution. During the discharge reaction, only one broad peak potential at  $\sim 3.94 \text{ V}$  is noted instead of two oxidation peaks ( $\sim 4.14$  and  $\sim 4.48 \text{ V}$ ). This corroborates the reversible insertion of two moles of lithium by forming solid-solution and is well reflected in monotonous discharge curves. Third lithium is inserted by two step process and exhibiting prominent sharp peak potentials at  $\sim 3.58$  and  $3.49 \text{ V}$  and



**Figure 7.** Cyclic voltammetric (CV) curves of  $\text{Li/C-Li}_3\text{V}_{1.98}\text{Al}_{0.02}(\text{PO}_4)_3$  (0.15 moles of adipic acid) cycled at slow scan rate of  $0.05 \text{ mV s}^{-1}$  between 3–4.8 V vs. Li, in which metallic lithium acts as both counter and reference electrodes.



**Figure 8.** Electrochemical impedance spectra of bare and carbon coated  $\text{Li}_3\text{V}_{1.98}\text{Al}_{0.02}(\text{PO}_4)_3$ .

obeying two-phase reaction. This was clearly evident from the short flat potential discharge curves by galvanostatic measurement.

To establish the influence of carbon coating on electronic conductivity profiles of NASICON type  $\text{Li}_3\text{V}_{1.98}\text{Al}_{0.02}(\text{PO}_4)_3$  phase, an electrochemical impedance spectroscopy (EIS) was performed and the obtained Nyquist plot is presented in Figure 8. Nyquist plot composed of semicircle and followed by a vertical tail inclined at  $45^\circ$ . Generally, high-frequency region is ascribed to the formation of surface films (preferably the decomposition of electrolyte solution and forming of by-products over the active material surface) and/or contact resistance. Medium frequency region is assigned to the charge-transfer (CT) resistance across the electrode/electrolyte interface and the long vertical tail inclined to the real axis corresponds to the lithium diffusion kinetics called Warburg tail.<sup>33</sup> It is apparent from the plot that a decrease in CT resistance for  $\text{C-Li}_3\text{V}_{1.98}\text{Al}_{0.02}(\text{PO}_4)_3$  compared to bare  $\text{Li}_3\text{V}_{1.98}\text{Al}_{0.02}(\text{PO}_4)_3$ . The decrease in CT value is correlated to an increase in electronic conductivity after in-situ carbon coating and presence of carbon layer was well demonstrated in the electrochemical properties of  $\text{Li}_3\text{V}_{1.98}\text{Al}_{0.02}(\text{PO}_4)_3$ .

## Conclusions

To summarize, metal (Mn, Fe and Al) doping and its optimization was successfully conducted on vanadium site of NASICON type  $\text{Li}_3\text{V}_2(\text{PO}_4)_3$  by solid-state reaction under Ar atmosphere. Among the various metal doping 0.02 mol concentration of Al on vanadium site ( $\text{Li}_3\text{V}_{1.98}\text{Al}_{0.02}(\text{PO}_4)_3$ ) resulted in high performance cathode and exhibited the reversible capacity of  $\sim 166 \text{ mAh g}^{-1}$  (2.53 moles of lithium) at current density of  $0.1 \text{ mA cm}^{-2}$ . To further improve the reversible capacity, carbon coating was conducted for  $\text{Li}_3\text{V}_{1.98}\text{Al}_{0.02}(\text{PO}_4)_3$  by using adipic acid as precursor. The presence of carbon coating was validated through TEM and Raman analysis. Based on the optimization, 0.15 moles of adipic acid was found to yield better performing electrode ( $\text{C-Li}_3\text{V}_{1.98}\text{Al}_{0.02}(\text{PO}_4)_3$ ) and showed the discharge capacity of  $\sim 182 \text{ mAh g}^{-1}$  (2.77 moles of lithium) at current density of  $0.1 \text{ mA cm}^{-2}$ . Further,  $\text{Li/C-Li}_3\text{V}_{1.98}\text{Al}_{0.02}(\text{PO}_4)_3$  cell retained 85% (2.36 moles of lithium) of its initial capacity after 40 galvanostatic cycles between 3–4.8 V vs. Li. These results provide the possibility of using higher capacity, 4 V, polyanion framework  $\text{C-Li}_3\text{V}_{1.98}\text{Al}_{0.02}(\text{PO}_4)_3$  cathodes in Li-ion batteries in the future.

## Acknowledgment

This work was supported by Energy Efficiency and Resources R&D program (20112010100150) under the Ministry of Knowledge Economy, Republic of Korea.

## References

1. M.-K. Song, S. Park, F. M. Alamgir, J. Cho, and M. Liu, *Materials Science and Engineering: R: Reports*, **72**(11), 203 (2011).
2. O. K. Park, Y. Cho, S. Lee, H.-C. Yoo, H.-K. Song, and J. Cho, *Energy & Environmental Science*, **4**(5), 1621 (2011).
3. V. Aravindan, J. Gnanaraj, S. Madhavi, and H. K. Liu, *Chemistry - A European Journal*, **17**(51), 14326 (2011).
4. J. B. Goodenough and Y. Kim, *Chemistry of Materials*, **22**(3), 587 (2009).
5. M. Y. Saïdi, J. Barker, H. Huang, J. L. Swayer, and G. Adamson, *Journal of Power Sources*, **119–121**, 266 (2003).
6. A. K. Padhi, K. S. Nanjundaswamy, and J. B. Goodenough, *J. Electrochem. Soc.*, **144**(4), 1188 (1997).
7. K. S. Nanjundaswamy, A. K. Padhi, J. B. Goodenough, S. Okada, H. Ohtsuka, H. Arai, and J. Yamaki, *Solid State Ionics*, **92**(1–2), 1 (1996).
8. A. K. Padhi, K. S. Nanjundaswamy, C. Masquelier, S. Okada, and J. B. Goodenough, *Journal of The Electrochemical Society*, **144**(5), 1609 (1997).
9. A. K. Padhi, K. S. Nanjundaswamy, C. Masquelier, and J. B. Goodenough, *Journal of The Electrochemical Society*, **144**(8), 2581 (1997).
10. C. Masquelier, A. K. Padhi, K. S. Nanjundaswamy, and J. B. Goodenough, *Journal of Solid State Chemistry*, **135**(2), 228 (1998).
11. V. Aravindan, W. Chuiling, M. V. Reddy, G. V. S. Rao, B. V. R. Chowdari, and S. Madhavi, *Physical Chemistry Chemical Physics*, **14**(16), 5808 (2012).
12. Z. Gong and Y. Yang, *Energy & Environmental Science*, **4**(9), 3223 (2011).
13. S. K. Martha, B. Markovsky, J. Grinblat, Y. Gofer, O. Haik, E. Zinigrad, D. Aurbach, T. Drezen, D. Wang, G. Deghenghi, and I. Exnar, *Journal of the Electrochemical Society*, **156**(7), A541 (2009).
14. C. Ouyang, S. Shi, Z. Wang, X. Huang, and L. Chen, *Physical Review B*, **69**(10), 104303 (2004).
15. G. Ting-Kuo Fey, T.-L. Lu, F.-Y. Wu, and W.-H. Li, *Journal of Solid State Electrochemistry*, **12**(7), 825 (2008).
16. V. Aravindan, S. Ravi, W. S. Kim, S. Y. Lee, and Y. S. Lee, *Journal of Colloid and Interface Science*, **355**(2), 472 (2011).
17. H. H. Lim, I. C. Jang, S. B. Lee, K. Karthikeyan, V. Aravindan, and Y. S. Lee, *Journal of Alloys and Compounds*, **495**(1), 181 (2010).
18. S. C. Yin, H. Grondey, P. Strobel, M. Anne, and L. F. Nazar, *J. Am. Chem. Soc.*, **125**(34), 10402 (2003).
19. H. Huang, S. C. Yin, T. Kerr, N. Taylor, and L. F. Nazar, *Adv. Mater.*, **14**(21), 1525 (2002).
20. S. Patoux, C. Wurm, M. Morcrette, G. Rousse, and C. Masquelier, *Journal of Power Sources*, **119–121**(0), 278 (2003).
21. S. Patoux and C. Masquelier, *Chemistry of Materials*, **14**(12), 5057 (2002).
22. A. R. Cho, J. N. Son, V. Aravindan, H. Kim, K. S. Kang, W. S. Yoon, W. S. Kim, and Y. S. Lee, *Journal of Materials Chemistry*, **22**(14), 6556 (2012).
23. Y. L. Cheah, V. Aravindan, and S. Madhavi, *ACS Applied Materials & Interfaces*, **4**(6), 3270 (2012).
24. A. C. Ferrari and J. Robertson, *Physical Review B*, **61**(20), 14095 (2000).
25. V. Aravindan, K. Karthikeyan, S. Amaresh, and Y. S. Lee, *Bulletin of the Korean Chemical Society*, **31**(6), 1506 (2010).
26. C. G. Son, H. M. Yang, G. W. Lee, A. R. Cho, V. Aravindan, H. S. Kim, W. S. Kim, and Y. S. Lee, *Journal of Alloys and Compounds*, **509**(4), 1279 (2011).
27. V. Aravindan, K. Karthikeyan, K. S. Kang, W. S. Yoon, W. S. Kim, and Y. S. Lee, *Journal of Materials Chemistry*, **21**(8), 2470 (2011).
28. V. Aravindan, K. Karthikeyan, S. Ravi, S. Amaresh, W. S. Kim, and Y. S. Lee, *Journal of Materials Chemistry*, **20**(35), 7340 (2010).
29. Y. N. Ko, H. Y. Koo, J. H. Kim, J. H. Yi, Y. C. Kang, and J.-H. Lee, *Journal of Power Sources*, **196**(16), 6682 (2011).
30. H. Liu, P. Gao, J. Fang, and G. Yang, *Chemical Communications*, **47**(32), 9110 (2011).
31. P. Fu, Y. Zhao, Y. Dong, X. An, and G. Shen, *Journal of Power Sources*, **162**(1), 651 (2006).
32. A. Tang, X. Wang, and Z. Liu, *Materials Letters*, **62**(10–11), 1646 (2008).
33. K. Yang, Z. Deng, and J. Suo, *Journal of Power Sources*, **201**(0), 274 (2012).